Structural Evolution of a Colloidal Crystal Fiber during Heating and Annealing Studied by in Situ Synchrotron Small Angle X-ray Scattering

ARTICLE *in* LANGMUIR · AUGUST 2010

Impact Factor: 4.46 · DOI: 10.1021/la102258b · Source: PubMed

8 AUTHORS, INCLUDING:

Jens Rieger
Harvard University
55 PUBLICATIONS **1,740** CITATIONS
SEE PROFILE

Stephan V Roth
Deutsches Elektronen-Synchrotron
364 PUBLICATIONS **3,273** CITATIONS
SEE PROFILE

Rainer Gehrke
Deutsches Elektronen-Synchrotron
170 PUBLICATIONS **1,573** CITATIONS
SEE PROFILE

Yongfeng Men
Chinese Academy of Sciences
86 PUBLICATIONS **1,406** CITATIONS
SEE PROFILE

Langmuir
Article

pubs.acs.org/Langmuir

Structural Evolution of a Colloidal Crystal Fiber during Heating and Annealing Studied by in Situ Synchrotron Small Angle X-ray Scattering

Shanshan Hu,[†,⊥] Jens Rieger,[‡] Zhiyong Yi,[†] Jianqi Zhang,[†] Xuelian Chen,[†] Stephan V. Roth,[§] Rainer Gehrke,[§] and Yongfeng Men*[,†]

[†] *State Key Laboratory of Polymer Physics and Chemistry, Changchun Institute of Applied Chemistry, Chinese Academy of Sciences, Graduate School of Chinese Academy of Sciences, Renmin Street 5625, 130022 Changchun, P. R. China,* [‡] *BASF SE, Polymer Research, 67056 Ludwigshafen, Germany, and* [§] *HASYLAB am DESY, Notkestrasse 85, 22607 Hamburg, Germany.* [⊥] *Current address: School of Chemistry and Chemical Engineering, Southwest University, 400715 Chongqing, P. R. China*

Received June 4, 2010. Revised Manuscript Received July 2, 2010

The structural evolution of a colloidal crystal fiber during heating and annealing was followed by in situ synchrotron small-angle X-ray scattering. The polymer dispersion (with a particle size of 118 nm) from which the fibers were formed by directed drying contained emulsifier and salt. A cellular structure formed upon drying in which the percolating phase (the "membrane phase") is composed from these components; this membrane phase gives rise to the scattering contrast on which the present observations build. Changes of the lattice constant of the colloidal crystallites and the intensity evolution of the scattering from the crystalline and the amorphous phases during heating and annealing indicate characteristic temperatures where the system exhibits pronounced structural changes. The first characteristic temperature was identified as 125 °C above which residue water in the membrane material was evaporated leading to shrinkage of the colloidal crystalline lattice. At a temperature above about 140 °C the membrane material was expelled out of the crystalline domains. This effect is accompanied by the progressive interdiffusion of polymer chains between adjacent latex particles and leads to further thermal shrinkage of the colloidal crystals. The second characteristic temperature is defined by a rapid increase in isotropic scattering. This effect is attributed to the formation of increasingly large domains of the membrane material and the concomitant disappearance of the membrane phase from the former crystal domains.

Introduction

Polymer dispersions made of compact polymeric particles with a typical size of around 100 nm are widely applied in paints, paper coatings, water-based adhesives, etc. Film formation of such dispersions usually refers to the process of evaporation of water accompanied by particle ordering, particle deformation, and interdiffusion of the constituting polymers across the particle boundaries.[1−3] After the completion of interdiffusion, all traces of the original matrix structure will eventually be lost. It has been suggested that polymer chains must diffuse from one particle into the neighboring ones in order to form a strong and continuous film. However, the investigation of polymer diffusion was hampered for a long time because of the lack of suitable measuring techniques. The interdiffusion of polymer molecules in latex films was finally proven by small-angle neutron-scattering (SANS),[4−7] nonradiative energy transfer methods,[8−10] and atomic force microscopy (AFM).[11−14] In SANS experiments the interdiffusion behavior was studied by measurements on latex blends made from deuterated latex particles, while in fluorescence investigations polymer diffusion was studied by direct nonradiative energy transfer measurements using latex films comprising two types of particles, one labeled with a donor dye and the other with an acceptor. AFM was used to analyze the surface topography of the latex thin films during thermal treatment. The speed of interdiffusion between latex particles depends on the structure and chemistry of the particle surfaces and the resulting cell walls as well as on the temperature—and, of course, on the chemistry and molar mass distribution of the polymers making up the dispersion particles. It may be envisaged that the outer hydrophilic layers or "shells" of polymer particles creates a continuous membrane that retards or prevents interdiffusion in latex films. More advanced studies about interdiffusion have been performed, including studies on the effect of molar mass,[10,15] polymer composition,[16,17] the influence of coalescing aids[18] and surfactants,[13,19]

*Corresponding author. E-mail: men@ciac.jl.cn.

(1) Keddie, J. L *Mater. Sci. Eng. R* **1997**, *21*, 101–170.
(2) Steward, P. A.; Hearn, J.; Wilkinson, M. C. *Adv. Colloid Interface Sci.* **2000**, *86*, 195–267.
(3) Winnik, M. A. *Curr. Opin. Colloid Interface Sci.* **1997**, *2*, 192–199.
(4) Hahn, K.; Ley, G.; Schuller, H.; Oberthur, R. *Colloid Polym. Sci.* **1986**, *264*, 1092–1096.
(5) Joanicot, M.; Wong, K.; Cabane, B. *Macromolecules* **1996**, *29*, 4976–4984.
(6) Joanicot, M.; Wong, K.; Richard, J.; Maquet, J.; Cabane, B. *Macromolecules* **1993**, *26*, 3168–3175.
(7) Rieger, J.; Hadicke, E.; Ley, G.; Lindner, P. *Phys. Rev. Lett.* **1992**, *68*, 2782–2785.
(8) Zhao, C. L.; Wang, Y. C.; Hruska, Z.; Winnik, M. A. *Macromolecules* **1990**, *23*, 4082–4087.
(9) Kim, H. B.; Winnik, M. A. *Macromolecules* **1995**, *28*, 2033–2041.
(10) Oh, J. K.; Tomba, P.; Ye, X. D.; Eley, R.; Rademacher, J.; Farwaha, R.; Winnik, M. A. *Macromolecules* **2003**, *36*, 5804–5814.
(11) Lin, F.; Meier, D. J. *Langmuir* **1995**, *11*, 2726–2733.
(12) Perez, E.; Lang, J. *Macromolecules* **1999**, *32*, 1626–1636.
(13) Aramendia, E.; Mallegol, J.; Jeynes, C.; Barandiaran, M. J.; Keddie, J. L.; Asua, J. M. *Langmuir* **2003**, *19*, 3212–3221.
(14) Goudy, A.; Gee, M. L.; Biggs, S.; Underwood, S. *Langmuir* **1995**, *11*, 4454–4459.
(15) Boczar, E. M.; Dionne, B. C.; Fu, Z. W.; Kirk, A. B.; Lesko, P. M.; Koller, A. D. *Macromolecules* **1993**, *26*, 5772–5781.
(16) Liu, Y. Q.; Haley, J. C.; Deng, K.; Lau, W.; Winnik, M. A. *Macromolecules* **2007**, *40*, 6422–6431.
(17) Wang, Y. C.; Winnik, M. A. *Macromolecules* **1993**, *26*, 3147–3150.
(18) Juhue, D.; Wang, Y. C.; Winnik, M. A.; Haley, F. *Makromol. Chem., Rapid Commun.* **1993**, *14*, 345–349.
(19) Ye, X. D.; Wu, J.; Oh, J. K.; Winnik, M. A.; Wu, C. *Macromolecules* **2003**, *36*, 8886–8889.

Scheme 1. Schematic Representation of the Foamlike Structure of Colloidal Crystalline Latex Film

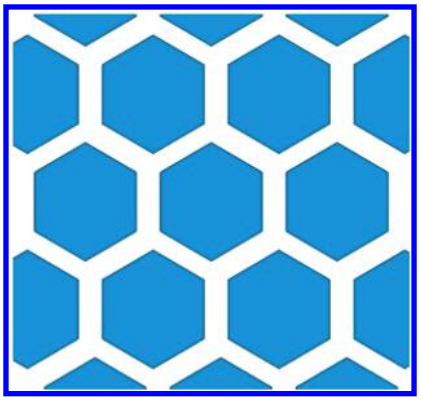

and on the influence of latex structure on the interdiffusion process.[9,20] Recently, the effect of annealing on the deformation mechanism in latex films was investigated by in situ synchrotron small-angle X-ray scattering (SAXS) technique.[21]

In previous work we investigated the film formation process of a styrene/*n*-butyl acrylate copolymer latex dispersion at room temperature by means of in situ SAXS technique.[22] Upon water evaporation, particle ordering and particle deformation until complete drying was observed, i.e., no polymer interdiffusion between adjacent particles occurred at room temperature. It has been speculated that this is due to the chemical nature of the surface of the latex particles. To promote the interdiffusion of the polymeric chains in the latex film, annealing at a sufficiently high temperature is required.

The polymer dispersion-based film used in this work exhibits a fiber symmetric face centered cubic (fcc) colloid crystal structure showing a large number of diffraction spots in SAXS experiments. The advantage of using this sample is that the scattering from the amorphous phase and diffraction from the crystalline phase can be easily separated. As will be shown in the following sections, the evolution of the interplanar distance of the fcc structure and the scattering intensity yields information about polymer interdiffusion and the coarsening of interparticle membranes during thermal treatment.

Experimental Section

A styrene/*n*-butyl acrylate copolymer (T_g = 20 °C) polymer dispersion was used in this study. The average particle diameter is 118 nm. Details about this latex dispersion can be found elsewhere.[21−23] The dispersion contains additional emulsifier, salt, etc., which usually form a continuous layer around the deformed particles after drying.[5,6] A foamlike structure is formed in which the continuous layer acts as cell wall or membrane as is shown in Scheme 1.

The latex film was obtained by evaporating water from a 25 wt % latex dispersion in a cuboidal Kapton tube with a length of 25 mm, a width of 5 mm, and a height of 1.5 mm. The evaporation process is nearly the same as during drying in a cylindrical tube;[23] the system starts to solidify at one side of the tube, whereas the dispersion on the other side remains liquid and retracts to the inside. In this work, the dispersion was dried at 25 ± 1 °C at a relative humidity of 30 ± 5% for 2 weeks, yielding a transparent film with dimensions of about 5 × 5 × 1 mm^3.

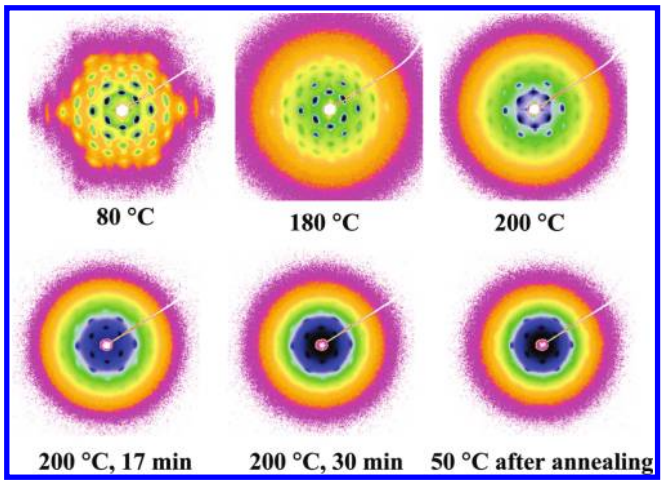

Figure 1. Selected 2D SAXS patterns obtained during heating and annealing of the latex film.

Online thermal synchrotron SAXS measurements were carried out at BW4, HASYLAB at DESY, Hamburg, Germany. The film was packed in a thin aluminum foil and then mounted onto a vacuum thermal stage. The sample was first heated up from 80 to 200 °C at a heating rate of 2 K/min. Then the sample was kept at 200 °C for 30 min before it was cooled down to 50 °C. The X-ray wavelength was λ = 0.13808 nm. The size of the primary X-ray beam at the sample position was 0.4 × 0.4 mm^2. The sample to detector distance was 5694 mm. The effective scattering vector **q** (**q** = $(4\pi/\lambda)\sin\theta$, where 2θ is the scattering angle and λ is the wavelength) range was 0.03−0.6 nm^{-1}. SAXS patterns were collected with an exposure time of 20 s every 30 s with a CCD camera (1024 pixels × 1024 pixels, pixel size: 158.2 μm). The SAXS data were calibrated for background scattering and normalized with respect to the primary beam intensity.

To observe the change in weight during heating and annealing of the colloidal crystalline latex film, thermal gravimetric analysis (TGA) measurement under the same temperature protocol as in the SAXS measurements was performed in a thermogravimetric analyzer (TGA/DSC 1) of Mettler Toledo, Swiss.

Results and Discussion

Selected SAXS patterns during annealing are shown in Figure 1. The temperatures and/or the annealing time at 200 °C are indicated at each pattern. The diffraction pattern taken at 80 °C reveals that the sample used in this experiment consists of fiber symmetric colloidal crystals. The diffraction peaks can be readily indexed to Bragg positions of a uniaxially oriented fcc lattice, as explained in more detail in a previous paper.[23] It was observed that the growth of the fiber symmetric colloidal crystals is not affected by the shape of the container but dominantly controlled by the evaporation mode, which also provides the breaking of symmetry necessary to induce the fiber symmetric arrangement of the crystals. Figure 1 shows that during heating and annealing all diffraction spots become weaker and the spots located at higher **q**-values even disappear finally. The disappearance of the diffraction spots indicates that the original crystalline matrix structure is gradually lost due to polymer interdiffusion.

To compare the changes in the scattering intensity of the latex film during heating and annealing the 2D SAXS patterns were integrated over all azimuthal angles yielding 1D intensity distributions shown in Figure 2. The intensity distribution measured during heating from 80 to 170 °C only decreased slightly. If there were only a crystalline phase in the system, solely, the diffraction peaks would be detected. But the integrated curves in Figure 2 show an increase of the total scattering intensity beyond 170 °C

(20) Juhue, D.; Lang, J. *Macromolecules* **1995**, *28*, 1306–1308.
(21) Zhang, J. Q.; Hu, S. S.; Rieger, J.; Roth, S. V.; Gehrke, R.; Men, Y. F. *Macromolecules* **2008**, *41*, 4353–4357.
(22) Hu, S. S.; Rieger, J.; Lai, Y. Q.; Roth, S. V.; Gehrke, R.; Men, Y. F. *Macromolecules* **2008**, *41*, 5073–5076.
(23) Hu, S. S.; Men, Y. F.; Roth, S. V.; Gehrke, R.; Rieger, J. *Langmuir* **2008**, *24*, 1617–1620.

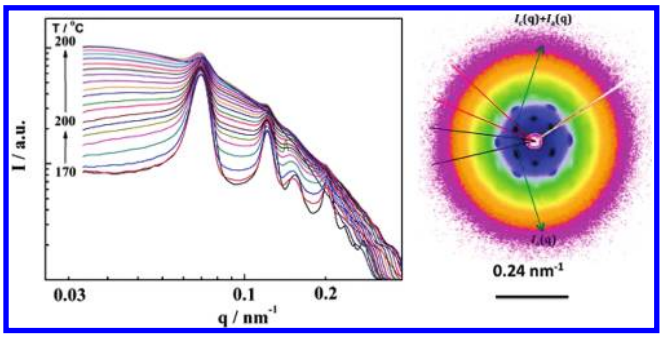

Figure 2. Integrated 1D SAXS data plotted for various annealing temperatures and times (left). Scheme indicating from which parts of the scattering pattern the scattering contributions are derived by integration (right).

even though the diffraction peaks become weaker. Therefore, it is safe to assume that the sample used in this experiment can be considered as a "two-phase" system: one phase is the crystalline phase of well-ordered packed particles and the other phase consists of domains of expelled membrane material. It is known that during annealing finally the cell walls break up and the polymers will interdiffuse freely. Hence the amorphous phase is composed of the expelled cell wall material outside of the crystalline domains consisting of fused latex particles.

In our scattering experiment, scattering intensities from the crystalline and amorphous phases were measured independently. The total scattering intensity is then given as the sum of the two contributions:

$$I(q) = I_c(q) + I_a(q) \quad (1)$$

$I_c(q)$ and $I_a(q)$ denote the scattering contributions from the crystalline and the amorphous regions. The scattering of the fiber symmetric crystals yields diffraction spots[23] while the scattering from amorphous phase results in rings.[22] Consequently, the experimental diffraction patterns consist of overlapping crystalline diffraction spots and amorphous rings. To separate the scattering from the crystalline phase and the amorphous phase, a simple approach was followed as described in Figure 2 (right). The arrows indicate regions of diffraction from 111 planes of the crystals and scattering from the amorphous phase, respectively. The scattering intensity distribution for the crystalline phase alone, $I_c(q)$, is obtained by subtracting from at the diffraction spots the scattering intensity of the amorphous phase at the corresponding q positions.

The interplanar distance in the colloidal crystals can be derived from the 1D scattering intensity distribution for the crystalline phase by using the Bragg equation $d_{hkl} = 2\pi/q_{hkl}$. To remove the effect of thermal expansion on the resultant interplanar distance, a linear thermal expansivity was obtained from the measured values of d_{hkl} at 200 °C before cooling down and after cooling down to 50 °C. The linear thermal expansivity a_l is calculated according to

$$a_l = \frac{l_t - l_0}{l_0 t} \quad (2)$$

where l_t and l_0 are the length of sample at the temperature of t and 0 °C, respectively. Microscopically, from eq 2, one obtains

$$d_{220}(t = 50) = \frac{d_{220}(t)}{1 + a_l(t - 50)}$$

The linear thermal expansivity a_l was determined as 2.9×10^{-4} K^{-1}. The interplanar distances at different temperatures were then related to a temperature of 50 °C to remove the effect of

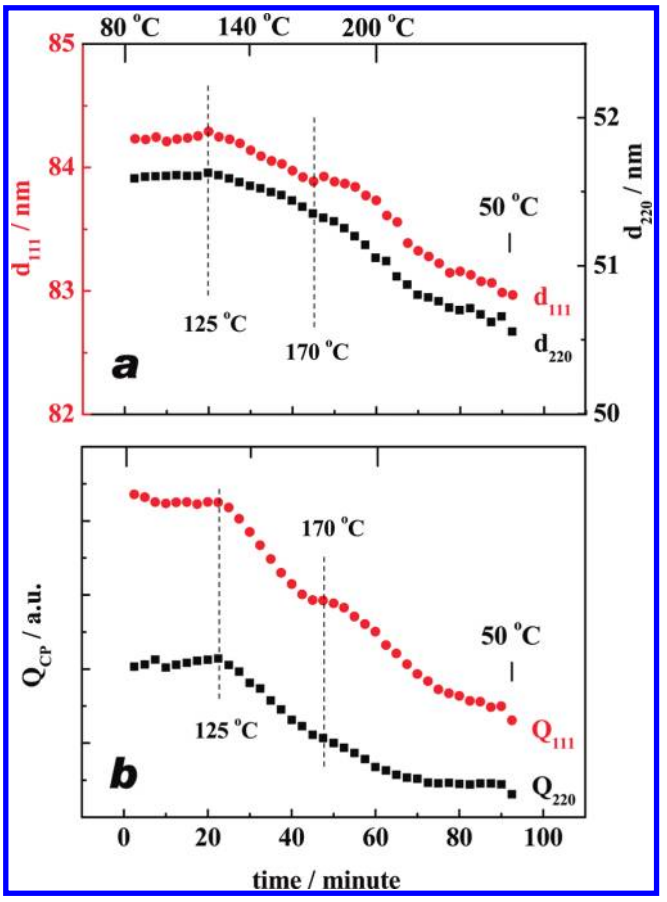

Figure 3. Interplanar distance of the 111 and 220 planes of the colloid crystals after subtracting the effect of thermal expansion (a) and integrated intensity of the [111] and [220] peaks plotted as a function of time (b).

thermal expansion. The interplanar distance of 111 and 220 planes in the crystalline phase after subtracting the effect of thermal expansion plotted as a function of time is given in Figure 3a. Without any loss of material from the crystalline phase during heating and annealing the values of d_{111} and d_{220} should stay constant. However, the interplanar distances are constant only below 125 °C and decrease upon further heating and annealing. The decrease of the interplanar distances indicates that the close-packed latex particles are getting even closer during annealing. In an effort of identifying the microscopic reasoning of this thermal shrinkage of colloidal crystalline lattice, weight loss of the latex film during heating and annealing was measured in a TGA test using same temperature protocol as in SAXS measurements. The TGA data together with the calculated changes in crystalline lattice volume based on the data presented in Figure 3 were shown in Figure 4. It must be mentioned that this direct comparison of volume and weight changes makes sense because the difference in density between different phases in the film is quite limited, being within a few percent. Changes in volume were obtained by considering an averaged lattice constant based on d_{111} and d_{220} values. In the TGA curve, a slight upturn was observed at the beginning of the heating process due to the slightly deformed baseline of the setup. Clearly, slight weight loss occurred when the temperature was raised from 120 to 140 °C. This effect can be attributed to the loss of residue water in the film due to the existence of salt and emulsifier. After this slight weight loss process, the system remained essentially unchanged in the TGA measurement. Thus, weight loss contributed to the thermal shrinkage of the colloidal crystalline lattice only at the beginning

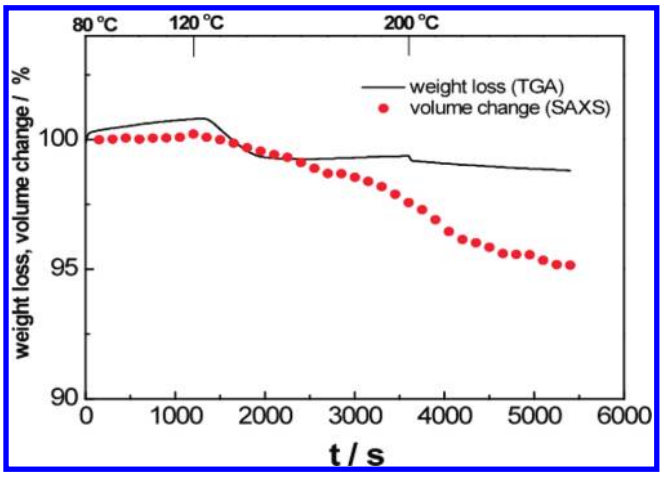

Figure 4. Weight loss derived from a TGA measurement and volume change in colloidal crystalline lattice obtained from SAXS data during heating and annealing.

of the whole process up to about 140 °C. Further shrinkage of the colloidal crystalline lattice can be explained by assuming that part of the membrane material was expelled out of the crystalline domains. The data reveal that the interplanar distance of the 220 plane decreased about 1 nm which means that the interparticle distance decreased about 2 nm after annealing.

The integrated scattering intensity of the [111] and [220] peaks, Q_{111} and Q_{220}, plotted as a function of time is shown in figure 3b. Q_{111} and Q_{220} are obtained by integrating the scattering intensity distributions of the pure crystalline phase (obtained as was described above) over respective **q** ranges covering the Bragg diffractions of (111) and (220) peaks. The evolution of the integrated intensity parallels the change of the interplanar distances. During heating from room temperature to 125 °C, the interplanar distance and the integrated intensity of the diffraction peaks remain essentially unchanged. When the temperature is higher than 125 °C, the distance and the intensity decrease continuously. It is well-known that the scattering power of the crystalline phase is given by[24]

$$Q_{CP} = V_c \Delta\rho_e^2 \phi_c (1-\phi_c) \propto \int_{\vartheta-\Delta\vartheta}^{\vartheta+\Delta\vartheta} \int_{q_\rho-\Delta q_\rho}^{q_\rho+\Delta q_\rho} I_c(\vartheta, q_\rho)\, \mathrm{d}\vartheta\, \mathrm{d}q_\rho$$

where V_c is the volume of crystalline phase irradiated by the X-rays, ϕ_c is the volume fraction of particles in the crystalline phase, $\Delta\rho_e$ is the electron density difference between the particles and the membrane material in the system, q_ρ is the position for integrating, and ϑ is the azimuthal angle. The values of $\Delta\vartheta$, q_ρ, and Δq_ρ have been chosen such that the crystal reflections are fully taken into account. According to this equation, the decrease of the intensity of crystalline phase is linked to two factors: one is the decrease of V_c resulting from the reduction of the number of particles in the crystalline phase because some particles merge; another is the decreasing of $\phi_c(1-\phi_c)$ caused by the increasing of the volume fraction of the particle in the crystalline phase, ϕ_c. Therefore, the diffracted intensity from the crystalline phase decreases continuously above 125 °C.

In some cases, interdiffusion will not occur until the membranes rupture. However the existence of a shell membrane does not necessarily mean that interdiffusion is prevented, it

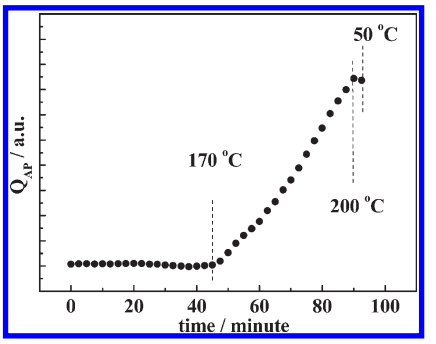

Figure 5. Scattering power of the amorphous phase as a function of time. The data were taken at a heating rate of 2 K/min.

Scheme 2. Schematic Representation of the Structural Features of the Colloidal Crystalline Latex Film during Heating and Annealing

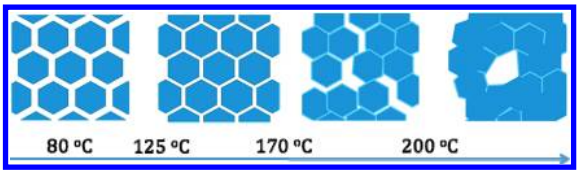

depends on the chemical composition of the membranes.[25,26] It is well-known that the effect of annealing on interdiffusion can be direct or indirect: annealing may increase the mobility of core polymers and allow them to pass through the membrane, or annealing may lead to a break-up of the membranes due to demixing and allow core polymers to interdiffuse freely.[5] Chevalier and co-workers concluded that the fragmentation of hydrophilic membranes and interdiffusion require mobility in both the membranes and in the cores.[27] Membranes without sufficient mobility will not break up, while cores without enough mobility will prevent expulsion of the membrane material.[6] In our case, the presence of membranes did not prevent interdiffusion, but only retarded it. Previous mechanical investigation showed that interdiffusion in the current system can occur at temperatures below 100 °C without changing the crystalline lattice constant.[21] It is thus clear that particle interdiffusion can be activated below 125 °C under the given heating conditions without changing the structure of membranes between particles.

In the present system, the fragmentation and coarsening of the membranes will lead to the expulsion of the membrane material. This will finally lead to an agglomeration of the membrane materials resulting in strong X-ray scattering toward small angles. An integration of such diffuse scattering indicates the scattering power of the irregular amorphous phase (Q_{AP}). In Figure 5, Q_{AP} as a function of time is presented. No scattering intensity from the amorphous phase is detected below 170 °C, but there is a strong increase above that temperature. This implies that the amount of merged particles and bulk membrane materials increases sharply above 170 °C. Above 170 °C, both the membrane material as well as the polymers in the particles gain sufficient mobility to allow for phase separation. If the annealing temperature is high enough or the heating time is long enough, the latex particles and the membranes are expected to separate completely; that is, all trace of the original matrix will be lost and the matrix material is completely expelled. To show the structuring process of the colloidal crystalline latex film, we present in Scheme 2 all stages of the structural evolution during heating and annealing.

(24) Glatter, O.; Kratky, O. *Small Angle X-ray Scattering*; Academic Press: London, 1982.
(25) Kim, H. B.; Wang, Y. C.; Winnik, M. A. *Polymer* **1994**, *35*, 1779–1786.
(26) Kim, H. B.; Winnik, M. A. *Macromolecules* **1994**, *27*, 1007–1012.
(27) Chevalier, Y.; Pichot, C.; Graillat, C.; Joanicot, M.; Wong, K.; Maquet, J.; Lindner, P.; Cabane, B. *Colloid Polym. Sci.* **1992**, *270*, 806–821.

Conclusions

The structural evolution of a colloidal crystalline latex film during heating and annealing was investigated by means of in situ synchrotron SAXS. The temperature dependence of the interplanar distance of the colloidal crystals and the evolution of scattering intensities of the crystalline and the amorphous phase upon heating were studied. Two transition temperatures of the structural evolution were identified. First, the interplanar distance remained constant below 125 °C but decreased upon further heating. Thus, local thermal shrinkage of the colloidal crystals was observed. The onset of the thermal shrinkage of the colloidal crystalline lattice can be attributed to the evaporation of residue water mixed with the membrane materials at the temperature below 140 °C. The membrane materials began to be expelled out of the crystalline matrix above 140 °C. At this temperature, the particles become mobile enough to expel the membrane material out of the matrix. Second, an increase of scattering intensity resulting from a phase separating amorphous phase was detected above 170 °C. The amorphous phase was composed of merged particles and bulk membrane material which starts to coalesce to a significant extent at 170 °C. Above this temperature, both the membrane material as well as the polymers making up the particles undergo larger scale phase separation.

Acknowledgment. We thank the National Science Foundation of China (Grants 20874101, 50921062) and HASYLAB project (II-20080190).